

The Effects of Ca^{2+} and MgADP on Force Development during and after Muscle Length Changes

Fabio C. Minozzo¹, Dilson E. Rassier^{1,2,3,4*}

1 Department of Kinesiology and Physical Education, McGill University, Montreal, Quebec, Canada, **2** Department of Physiology, McGill University, Montreal, Quebec, Canada, **3** Meakins-Christie Laboratories, McGill University, Montreal, Quebec, Canada, **4** Department of Physics, McGill University, Montreal, Quebec, Canada

Abstract

The goal of this study was to compare the effects of Ca^{2+} and MgADP activation on force development in skeletal muscles during and after imposed length changes. Single fibres dissected from the rabbit psoas were (i) activated in $\text{pCa}^{2+}4.5$ and $\text{pCa}^{2+}6.0$, or (ii) activated in $\text{pCa}^{2+}4.5$ before and after administration of 10 mM MgADP. Fibres were activated in sarcomere lengths (SL) of 2.65 μm and 2.95 μm , and subsequently stretched or shortened (5%SL at 1.0 $\text{SL}\cdot\text{s}^{-1}$) to reach a final SL of 2.80 μm . The kinetics of force during stretch were not altered by pCa^{2+} or MgADP, but the fast change in the slope of force development (P_1) observed during shortening and the corresponding SL extension required to reach the change (L_1) were higher in $\text{pCa}^{2+}6.0$ ($P_1 = 0.22 \pm 0.02 P_0$; $L_1 = 5.26 \pm 0.24 \text{ nm}\cdot\text{HS}^{-1}$) than in $\text{pCa}^{2+}4.5$ ($P_1 = 0.15 \pm 0.01 P_0$; $L_1 = 4.48 \pm 0.25 \text{ nm}\cdot\text{HS}^{-1}$). L_1 was also increased by MgADP activation during shortening. Force enhancement after stretch was lower in $\text{pCa}^{2+}4.5$ (14.9 \pm 5.4%) than in $\text{pCa}^{2+}6.0$ (38.8 \pm 7.5%), while force depression after shortening was similar in both Ca^{2+} concentrations. The stiffness accompanied the force behavior after length changes in all situations. MgADP did not affect the force behavior after length changes, and stiffness did not accompany the changes in force development after stretch. Altogether, these results suggest that the mechanisms of force generation during and after stretch are different from those obtained during and after shortening.

Citation: Minozzo FC, Rassier DE (2013) The Effects of Ca^{2+} and MgADP on Force Development during and after Muscle Length Changes. PLoS ONE 8(7): e68866. doi:10.1371/journal.pone.0068866

Editor: Miklos S. Kellermayer, Semmelweis University, Hungary

Received: December 14, 2012; **Accepted:** June 7, 2013; **Published:** July 16, 2013

Copyright: © 2013 Minozzo, Rassier. This is an open-access article distributed under the terms of the Creative Commons Attribution License, which permits unrestricted use, distribution, and reproduction in any medium, provided the original author and source are credited.

Funding: This work was supported by the Canadian Institutes of Health Research (CIHR) and Natural Sciences and Engineering Research Council of Canada (NSERC). The funders had no role in study design, data collection and analysis, decision to publish, or preparation of the manuscript.

Competing Interests: The authors have declared that no competing interests exist.

* E-mail: dilson.rassier@mcgill.ca

Introduction

Length changes imposed to activated muscles are commonly used to study the molecular mechanisms of contraction [1–6]. When muscle fibres are activated and subsequently stretched or shortened, force changes in four major steps: a fast rate of force change (phase 1) followed by a slower rate of force change (phase 2), after which the force stabilizes slowly (phase 3) to asymptotically return to a new steady state (phase 4) [4–6]. Although the mechanisms by which myosin crossbridges contribute to force changes observed during muscle stretch and shortening are still under investigation [7–12], phase 1 is commonly attributed to the elastic behavior of the crossbridges, and phase 2 is commonly associated with changes in the occupational fraction of crossbridges in the pre- and post- power-stroke states during the actomyosin cycle [5,6].

After stretch or shortening, force stabilizes at a higher or a lower level than that produced during isometric contractions at corresponding lengths, respectively (phase 4); these phenomena have been referred to as residual force enhancement and force depression [13–15]. Attempts to correlate these last-longing changes in force with changes that happen *during* length changes have proved inconclusive. It has been suggested that stretch can induce changes in crossbridge kinetics leading to a long-lasting increase in the number of crossbridges attached to actin [16], and that shortening can cause crossbridge deactivation due to newly overlap zone formed between myosin and actin filaments [15,17].

However, studies that measured stiffness – a putative measurement of crossbridges attached to actin – are contradictory; some show a direct relationship between stiffness and residual force changes [18,19] and others fail to find any correlation between the two variables [14,20].

The events dominating crossbridge kinetics during muscle stretch and shortening, and their potential relation with the residual force enhancement and depression need investigation. In this study, we approached this problem by investigating force during and after length changes (shortening and stretching) while altering either the population of attached crossbridges using different levels of Ca^{2+} activation, or biasing crossbridges into a strong-binding with actin by using MgADP activation [21]. Based on previous studies [6,22,23], we hypothesized that an increase in the number of crossbridges would not affect the relative forces produced during and after length changes, while changes in the crossbridges binding state would affect force during and after length changes. Confirmation of these hypotheses would link changes in crossbridge kinetics during length changes to the long-lasting effects observed in skeletal muscles.

Methods

Fibre Preparation

Muscle bundles (2–3 cm) from the rabbit psoas muscle were dissected, tied to wooden sticks, and chemically permeabilized as previously described [4,5]. Muscles were incubated in rigor

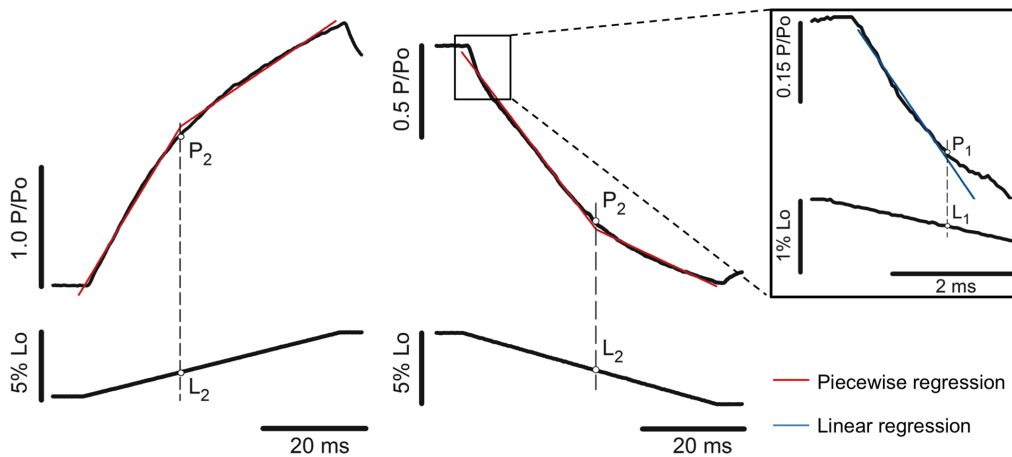


Figure 1. Detection of force transients during stretch and shortening of activated muscle fibres. Left-to-right: P₂ and L₂ detection during stretch and shortening, respectively. Force traces are on the top and fibre length variation at the bottom (P_o = isometric force; L_o = initial length). The force rise during stretch and the force decay during shortening can be fitted by two linear functions: $y_1 = a_1 + b_1 \times xi$ (restriction: $xi \leq x_o$) and $y_2 = a_2 + b_2 \times xi$ (restriction: $xi > x_o$), where (x_o, y_o) represents coordinates of the critical transitions (coordinates for P₂ in this case), a₁ and a₂ are the intercepts of the two regression lines, and b₁ and b₂ are the slopes of the two regression lines. The red traces in the graphs show the two-segmented piecewise regressions. The residual sum of squares (RSS) is based on the sum of the squares of each regression line: $RSS = \sum_{xi \leq x_o} [y_i - (a_1 + b_1 \times x_i)]^2 + \sum_{xi > x_o} [y_i - (a_2 + b_2 \times x_i)]^2$. RSS is used as a criterion to determine the optimal values of a₁, a₂, b₁, b₂, and x_o - those belonging to the minimal RSS are considered optimal. The blue trace displayed on the inset correspond to a simple linear regression, based on the best fit for the force coordinates (x_o, y_o) during the first 2–3 ms, and P₁ corresponds to the first data point where the regression does not follow the force trace. In both cases the statistic F-value and confidence intervals are calculated according to standard methods for regression analyses. L₁ and L₂ are extrapolated by crossing a perpendicular line passing by P₁ and P₂, respectively, until reaching the length traces. doi:10.1371/journal.pone.0068866.g001

solution (pH = 7.0) for approximately 4 hours, then transferred to a rigor:glycerol (50:50) solution for 15 hours, before storage in a fresh rigor:glycerol (50:50) solution containing a cocktail of protease inhibitors (Roche Diagnostics, USA) in a freezer (-20°C) for at least seven days. Prior to the experiment, one muscle sample was transferred to a fresh rigor solution to be defrosted in the fridge (4°C) for one hour before use. After cutting a small section (~4 mm in length) from the sample, single fibres were dissected in relaxing solution (pH = 7.0) and fixed with two aluminum foil clips. The fibres were placed inside a temperature-controlled chamber and attached between a force transducer

(Model 400A, Aurora Scientific, Toronto, Canada) and a length controller (Model 312B, Aurora Scientific, Toronto, Canada). The protocol was approved by the McGill University Animal Care Committee (protocol # 5227) and complied with the guidelines of the Canadian Council on Animal Care.

Solutions

The rigor solution (pH 7.0) was composed of (in mM): 50 Tris, 100 NaCl, 2 KCl, 2 MgCl₂, and 10 EGTA. The relaxing solution used for muscle storage and dissection (pH 7.0) was composed of (in mM): 100 KCl, 2 EGTA, 20 Imidazole, 4 ATP and 7 MgCl₂.

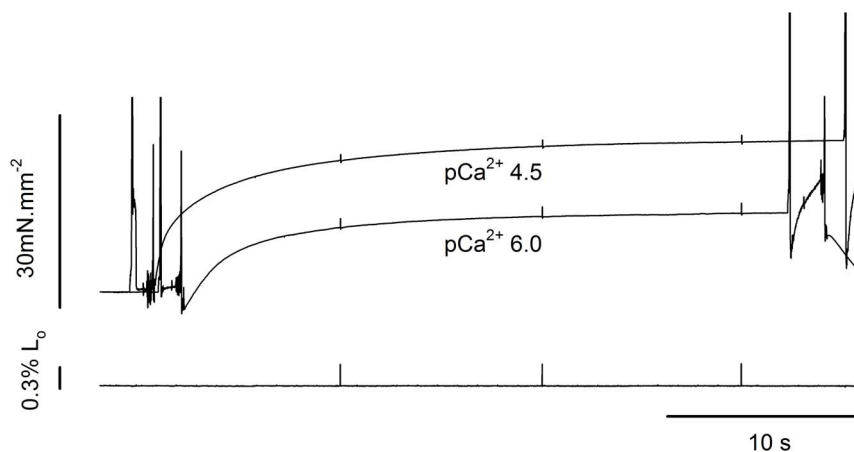


Figure 2. Superimposed isometric contractions in different Ca²⁺ concentrations. Sample records from typical isometric contractions produced in pCa²⁺4.5 and pCa²⁺6.0 (top), and corresponding length traces (bottom). The average sarcomere lengths in each contraction were 2.82 μm, and 2.83 μm, respectively. doi:10.1371/journal.pone.0068866.g002

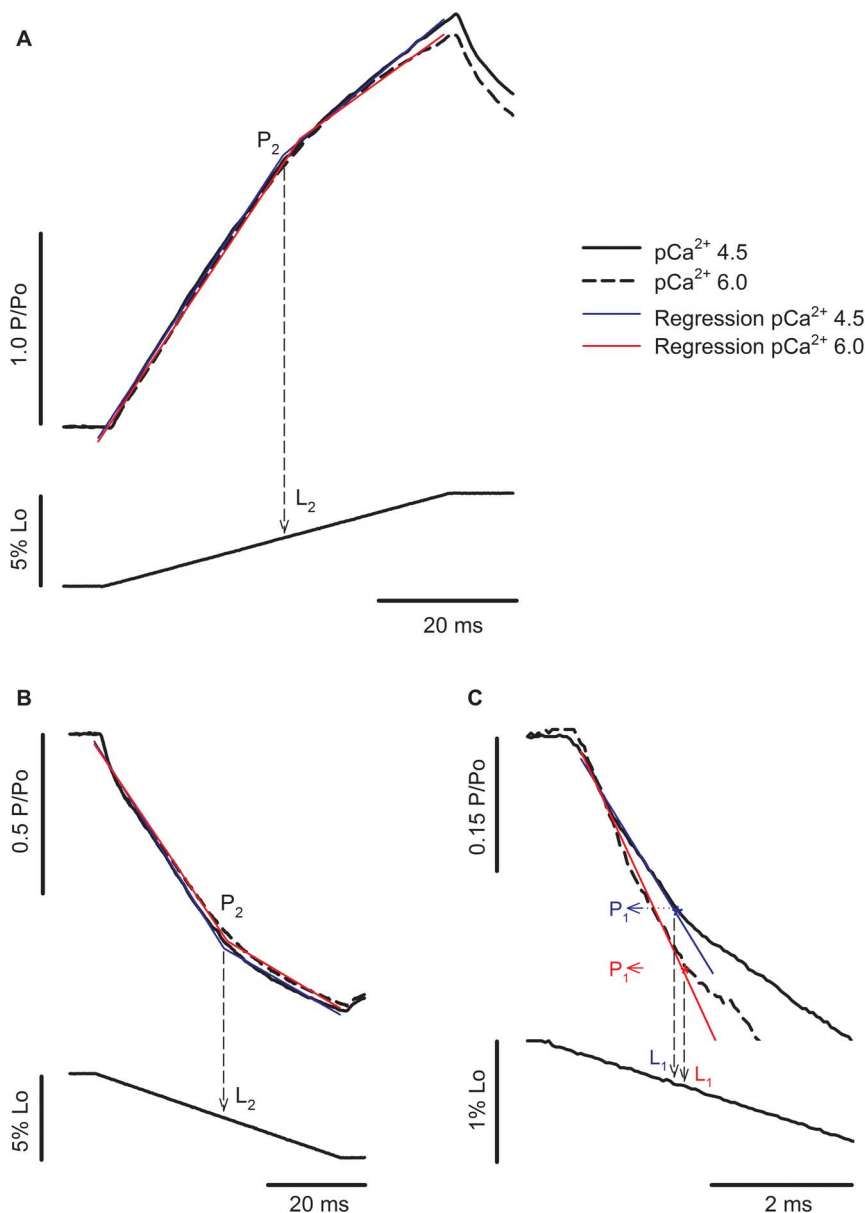


Figure 3. Force transients during length changes in different Ca^{2+} concentrations. (A) Superimposed contractions showing the force increase during stretch while the fibre was activated in pCa^{2+} 4.5 (solid line) and pCa^{2+} 6.0 (dashed line) (top), with corresponding changes in fibre length (bottom). All forces were normalized by the isometric forces (P_0) before the stretch. The regression lines for the contractions produced in pCa^{2+} 4.5 and pCa^{2+} 6.0 are shown in blue and red, respectively. (B) Superimposed contractions showing the force decrease during shortening when a fibre was activated in pCa^{2+} 4.5 (solid line) and pCa^{2+} 6.0 (dashed line) (top), with the corresponding length changes (bottom). (C) Closer view from the initial shortening phase, showing that decreasing Ca^{2+} concentration induced an increase in L_1 and P_1 amplitudes. All forces were normalized by the isometric forces (P_0) before the shortening. The regression lines for the contractions produced in pCa^{2+} 4.5 and pCa^{2+} 6.0 are shown in blue and red, respectively. Decreasing Ca^{2+} concentration increased L_1 and P_1 amplitude. doi:10.1371/journal.pone.0068866.g003

The experimental solutions with pCa^{2+} of 4.5, 6.0 and 9.0 (pH 7.0) contained (in mM): 20 imidazole, 14.5 creatine phosphate, 7 EGTA, 4 MgATP, 1 free Mg^{2+} , free Ca^{2+} in three concentration adjusted to obtain pCa^{2+} of 9.0, 6.0 and 4.5. KCl was used to adjust the ionic strength to 180 mM in all solutions. The final concentrations of each metal-ligand complex were calculated using a computer program based on Fabiato [24]. A pre-activating solution (pH 7.0; pCa^{2+} 9.0) with a reduced Ca^{2+} buffering capacity was used immediately prior to activation to minimize a delay in diffusion (in mM): 68 KCl, 0.5 EGTA, 20

Imidazole, 14.5 PCr, 4.83 ATP, 0.0013.7 CaCl_2 , 5.41 MgCl_2 and 6.5 HDTA. The MgADP solution was prepared by adding 0.214 g of MgADP to 50 mL of activation solution (pCa^{2+} 4.5), reaching a final MgADP concentration of 10 mM [15].

Experimental Protocol

The average sarcomere length (SL) of the fibres in the experimental chamber was calculated in relaxing solution using a high-speed video system (HVSL, Aurora Scientific 901A, Toronto, Canada). Images from a selected region of the fibres

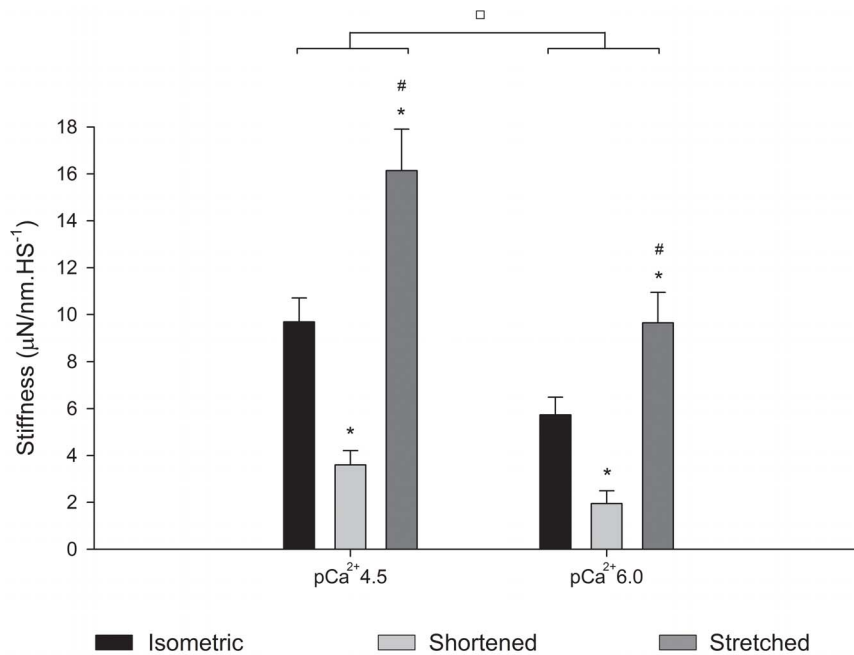


Figure 4. Mean stiffness values during length changes. Mean stiffness values (\pm S.E.M) during isometric contractions (black bar), shortening (light grey bar) and stretch (dark grey bar) from experiments performed in pCa²⁺4.5 and pCa²⁺6.0 (n = 13). Decreasing Ca²⁺ concentration significantly decreased the stiffness in all conditions. In both pCa²⁺, stiffness increased during stretch and decreased during shortening. * Significantly different from isometric, # significantly different from shortening, □ groups significantly different from each other. doi:10.1371/journal.pone.0068866.g004

were collected at 1000–1500 frames/second, and the SL was calculated using Fast Fourier Transform analysis based on the striation spacing produced by dark and light bands of myosin and actin, respectively. The fiber diameter and length were measured using a CCD camera (Go-3, QImaging, USA; pixel size: 3.2 $\mu\text{m} \times 3.2 \mu\text{m}$), and the cross-sectional area was estimated assuming circular symmetry.

Two separate sets of experiments were performed during this study: (i) fibres were activated in pCa²⁺4.5 and pCa²⁺6.0 (n = 13), or (ii) fibres were activated in pCa²⁺4.5 with or without MgADP (n = 7). Both sets of experiments followed the same procedures. Fibres were first activated to produce isometric contractions at nominal SLs of 2.65 μm , 2.80 μm and 2.95 μm . Fibres were subsequently activated at 2.65 μm and 2.95 μm , and a 5% SL change, at a speed of 1.0 SL.s⁻¹ (stretch or shortening, random order) was imposed after full force development, obtaining a final SL of 2.80 μm in both cases. In all trials, control contractions at SL of 2.80 μm were elicited at the end of the experiments, and if isometric forces decreased by >15% in relation to the first isometric contraction, or when the striation pattern corresponding to the SL became unclear, the experiments were ended and the data was not used.

During all experiments, fibre stiffness (k) was assessed three times during the contractions: after force was fully developed, but before length changes (30 s after activation started), immediately after the change in length and before the force was stabilized (40.0075 s after activation started), and after the force was stabilized following the length changes (50 s after activation started). Stiffness was evaluated by applying a fast length step ($dL = 0.3\% L_o$) to the fibres, and dividing the change in force during this step by the length change ($K = dF/dL$) [25].

Data Analysis

The force and stiffness obtained after stretch, after shortening and during the isometric reference contractions were compared between different conditions from each set of experiment; (i) fibres activated in pCa²⁺4.5 and 6.0, and (ii) fibres activated in pCa²⁺4.5 with or without MgADP. The changes in the slope of force traces observed while fibres were stretched and shortened were detected using a two-segment piecewise regression, as previously described [4,5]. The regression results were accepted when they presented a correlation coefficient (r^2) > 0.99. When this criterion was not met (a few cases for detection of P₁), we fitted a single linear regression in the data points spanning from the first 2–3 ms in which force started to change, since force is linear during this time [5,6]. The forces obtained at the first and second slope correspond to P₁ and P₂, and the SL amplitudes necessary to achieve P₁ and P₂ were named L₁ and L₂, respectively (Figure 1).

Statistics

A two-way analysis of variance (ANOVA) for repeated measures was used to compare the forces and stiffness values in the different experiments (pCa²⁺ and MgADP conditions), before and after length changes. ANOVA for repeated measures was also used to compare the values of P₁, P₂, L₁, and L₂ obtained during shortening and stretch in the different sets of experiments. When significant changes were observed, post-hoc analyses for multiple comparisons were performed with Newman-Keuls tests. A level of significance of $P \leq 0.05$ was set for all analyses. All values are presented as mean \pm S.E.M.

Results

Transient Forces during Length Changes

Experiments with different Ca²⁺ concentrations. Figure 2 shows two isometric contractions produced during a typical

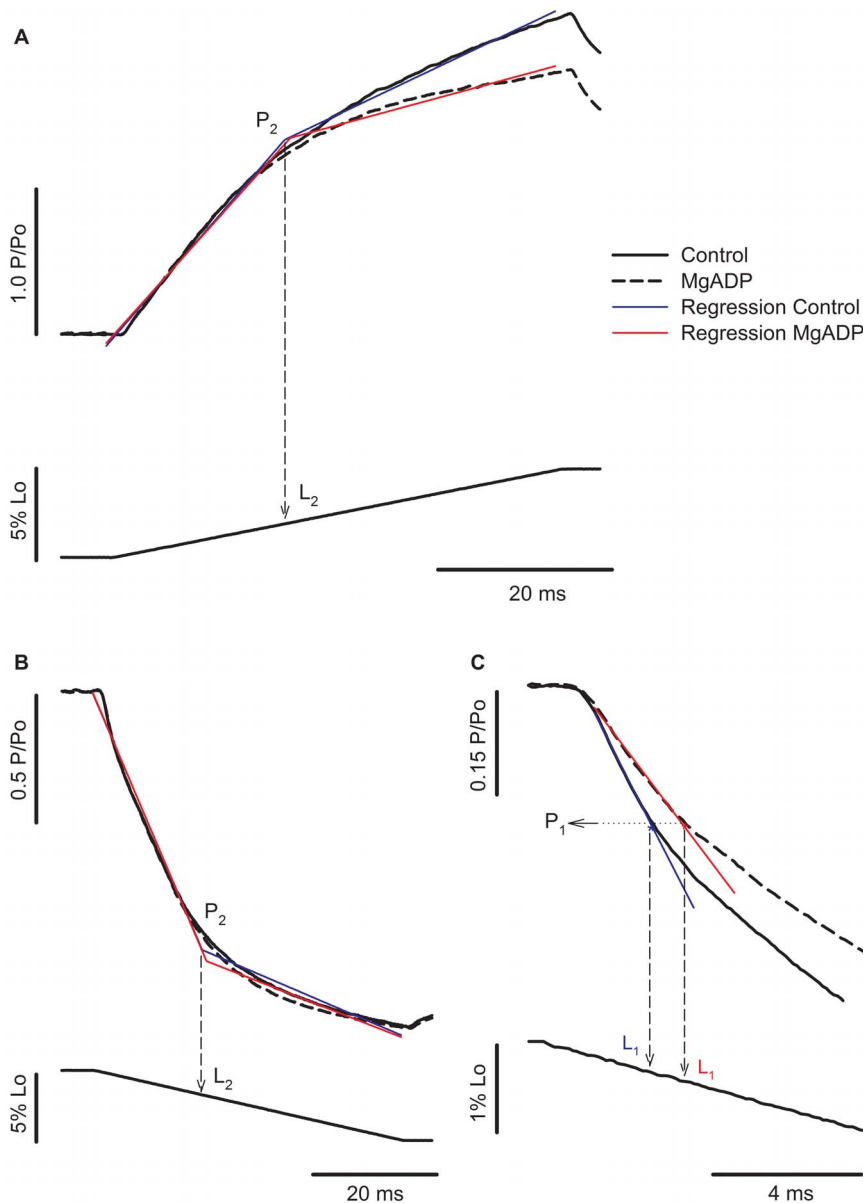


Figure 5. Force transients during length changes in fibres treated with MgADP. (A) Superimposed contractions showing the force increase during stretch (top) when the fibre was activated in $\text{pCa}^{2+}4.5$ (solid line) and treated with MgADP (dashed line). The corresponding length changes are shown in the bottom panels. All forces were normalized by the isometric forces (P_0) before the stretch. The regression lines for the contractions produced in $\text{pCa}^{2+}4.5$ and in presence of MgADP are shown in blue and red, respectively. (B) Superimposed contractions showing the force decrease during shortening (top) when a fibre was activated at $\text{pCa}^{2+}4.5$ (solid line) and treated with MgADP (dashed line). The corresponding changes in fibre length are shown in the bottom. (C) Closer view from the initial shortening phase showing that MgADP activation induced an increase in L_1 . All forces were normalized by the isometric forces (P_0) before the shortening. The regression lines for the contractions produced in $\text{pCa}^{2+}4.5$ before and after MgADP treatment are shown in blue and red, respectively. MgADP treatment increased L_1 significantly, while it did not change the other variables. doi:10.1371/journal.pone.0068866.g005

experiment in which a fibre was activated in $\text{pCa}^{2+}4.5$ and subsequently in $\text{pCa}^{2+}6.0$. The force produced in $\text{pCa}^{2+}4.5$ is in the range observed in previous studies that used permeabilized fibers from mammalian muscles activated at low temperatures (4–5°C). These studies show forces ranging from 48 to 58 mN/mm² when fibres contract at the plateau of the force-length relation [26–29]. Since we activated fibers on average sarcomere lengths between 2.7 μm and 2.9 μm , the force should be 20–30% lower than that produced at the plateau of the force-length relation, and thus our values are in close agreement with the literature. The force decreased when fibres were activated in $\text{pCa}^{2+}6.0$ by

$53.3 \pm 5.5\%$, similar to what has been reported in previous studies [4,5].

Figure 3 shows force and length traces recorded when a fibre was stretched or shortened in two different Ca^{2+} concentrations. The force was normalized by the maximum isometric force produced just before the stretch. The values of P_2 of 2.42 P_0 during stretch and 0.34 P_0 during shortening observed in this fibre, when activated in $\text{pCa}^{2+}4.5$, are in agreement with previous studies [3,6,12,30]. The value of L_2 observed during stretch was comparable with previous studies [31,32], but higher than what we observed before, where sarcomeres needed to be stretched by

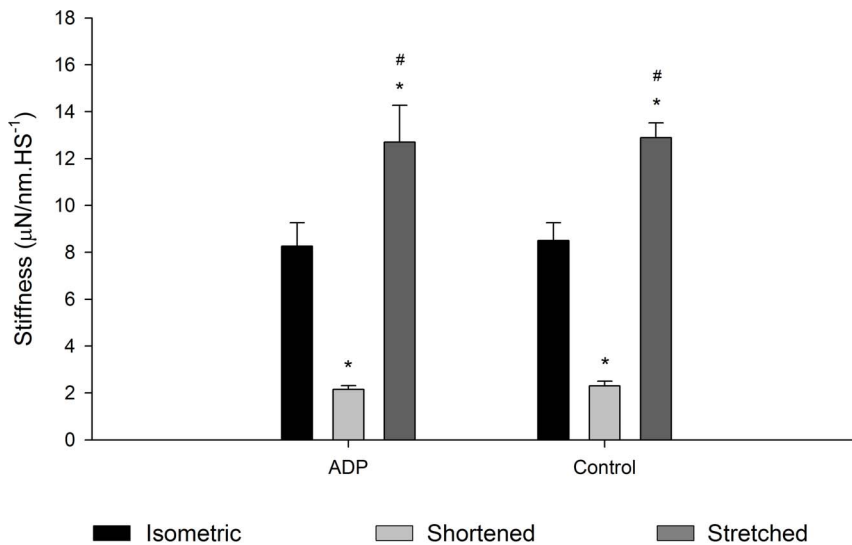


Figure 6. Mean stiffness values during length changes. Mean stiffness values (\pm S.E.M) during isometric contraction (black bar), shortening (light grey bar) and stretch (dark grey bar) obtained in experiments performed in pCa²⁺4.5 before and after MgADP treatment (n = 7). MgADP did not affect stiffness, but in stiffness was always increased during stretch and decreased during shortening. * Significantly different from isometric contractions, # significantly different from shortening. doi:10.1371/journal.pone.0068866.g006

~14 nm.HS⁻¹ before a change in the force trace was observed [4,33]. The difference may be related to the speed of stretch and SL, as in the previous study we used faster stretches at shorter SLs than used in the current experiments.

During stretch, P₂ and L₂ were not different between contractions performed in different pCa²⁺ (Figure 3A). We were unable to detect P₁ during stretch. However, during shortening, the P₁ amplitude (absolute distance between the P₁ and P_o, normalized by P_o) and L₁ were significantly higher in pCa²⁺6.0 than in pCa²⁺4.5 (Figure 3C). Note that the force does not reach a complete steady state just after shortening. The reasons for such behavior may vary, but it is likely associated with sarcomere length non-uniformities that develops with loaded shortening during full fiber activation and/or thin filament deactivation [6,34].

The stiffness decreased during shortening and increased during stretch (Figure 4). The relative stiffness increased less than the force during stretch in pCa²⁺4.5 and pCa²⁺6.0, but decreased similarly during shortening in both situations.

Experiments with MgADP. Figure 5 shows force and length traces recorded when a fibre was stretched before and after MgADP treatment. The force was normalized by the maximum isometric force produced before the stretch. P₂ and L₂ were not different between the two contractions (P₁ and L₁ were undetectable during stretch) (Figure 5A). Figure 5B and 5C shows force and length traces recorded during fibre shortening. L₁ was longer with the presence of MgADP, while all the other variables were not changed by MgADP (Figure 5C). The stiffness during length changes decreased during shortening and increased during stretch (Figure 6).

Table 1 summarizes the force and length transient values obtained in the two sets of experiments conducted in this study. Overall, during shortening P₁ decreased and L₁ increased at low Ca²⁺ concentration, whereas only L₁ increased when fibres were treated with MgADP.

Table 1. Force transients and respective half-sarcomere length extensions during stretch and shortening.

Length changes	Experiments	P ₁	P ₂	L ₁	L ₂	
Stretch	i) Effects of Ca ²⁺	pCa ²⁺ 4.5	-	2.51 ± 0.19	-	29.83 ± 1.45
		pCa ²⁺ 6.0	-	2.60 ± 0.14	-	30.37 ± 1.81
	ii) Effects of MgADP	Control (pCa ²⁺ 4.5)	-	2.48 ± 0.14	-	27.33 ± 0.70
		MgADP	-	2.47 ± 0.21	-	25.28 ± 1.71
Shortening	i) Effects of Ca ²⁺	pCa ²⁺ 4.5	0.85 ± 0.02	0.28 ± 0.04	4.48 ± 0.25	29.51 ± 1.67
		pCa ²⁺ 6.0	0.78 ± 0.02*	0.19 ± 0.07	5.26 ± 0.17*	30.17 ± 1.49
	ii) Effects of MgADP	Control (pCa ²⁺ 4.5)	0.80 ± 0.03	0.09 ± 0.14	4.34 ± 0.19	26.77 ± 0.94
		MgADP	0.78 ± 0.04	0.17 ± 0.09	5.52 ± 0.20*	26.73 ± 0.74

Legend: (i) Experiments performed with fibres activated in different Ca²⁺ concentrations (n = 13). (ii) Experiments performed with fibres treated with MgADP (n = 7). P₁ and P₂ correspond to the force/isometric force (P/P_o). L₁ and L₂ correspond to the half sarcomere extension obtained at P₁ and P₂, and are given in nm.HS⁻¹. * Significantly different from control. doi:10.1371/journal.pone.0068866.t001

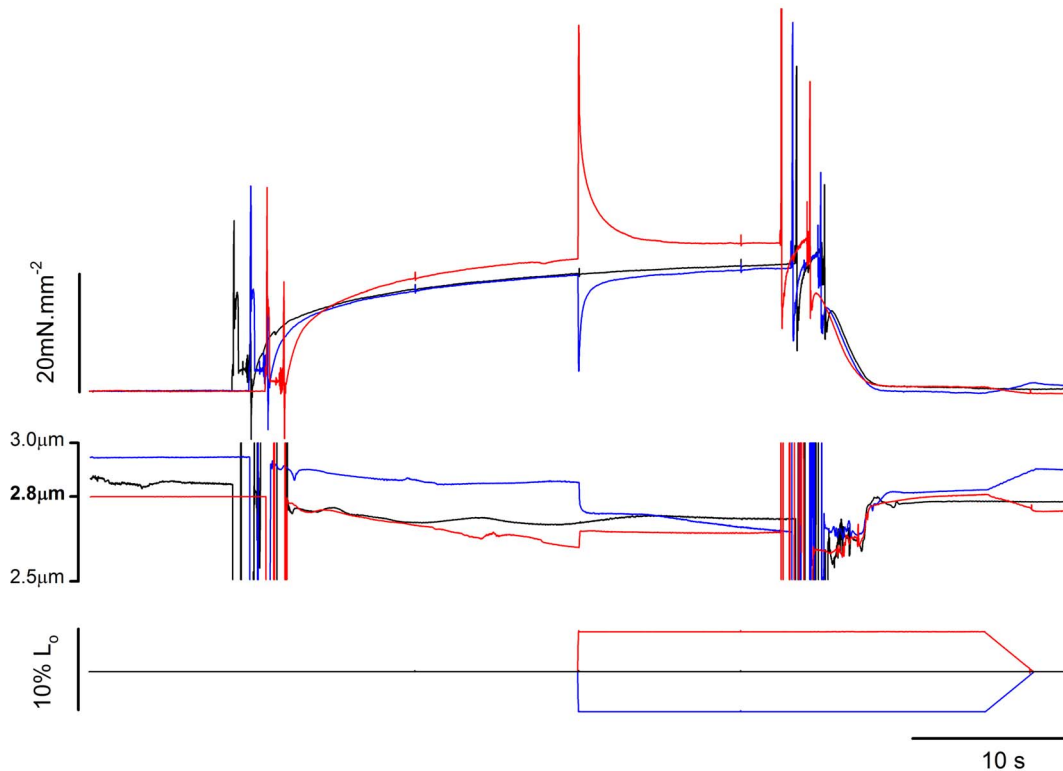


Figure 7. Typical experiment for analysis of residual force enhancement and force depression performed in $\text{pCa}^{2+}4.5$. Superimposed force traces (upper panel), SL traces (mid panel), and length traces (lower panel) from a fibre activated in $\text{pCa}^{2+}4.5$ and kept isometric (in black), stretched (in red), or shortened (in blue). doi:10.1371/journal.pone.0068866.g007

Residual Force Enhancement and Depression

Experiments with different Ca^{2+} concentrations. Figure 7 shows an experiment with three superimposed contractions produced in $\text{pCa}^{2+}4.5$ in different SLs. The steady-state isometric forces after stretch and shortening were higher and lower, respectively, than the force produced during the isometric contraction at the corresponding length, as shown before [6,14,18,35,36]. Changing Ca^{2+} concentration changed the levels of force enhancement (Figure 8A), such that the increase in force was higher when the fiber was activated and stretched in $\text{pCa}^{2+}6.0$ than in $\text{pCa}^{2+}4.5$. This result was confirmed statistically; although the absolute force enhancement ($4.2 \pm 0.8 \text{ mN} \cdot \text{mm}^{-2}$) was independent from pCa^{2+} , the relative enhancement was higher in $\text{pCa}^{2+}6.0$ ($38.8 \pm 7.4\%$) when compared to $\text{pCa}^{2+}4.5$ ($14.9 \pm 5.6\%$). Changing Ca^{2+} concentration did not change the effects of shortening on the long-lasting force; the residual force depression was similar in $\text{pCa}^{2+}4.5$ and $\text{pCa}^{2+}6.0$ (Figure 8B).

In order to test if the changes in the residual force as a result of pCa^{2+} could be attributed to variations in the number of crossbridges attached to actin, we compared the stiffness after length changes and during isometric contractions. Although the absolute stiffness was higher in $\text{pCa}^{2+}4.5$ (Figure 9), the stiffness enhancement after stretch was significantly larger in $\text{pCa}^{2+}6.0$ ($15.7 \pm 0.08\%$) than in $\text{pCa}^{2+}4.5$ ($6.4 \pm 0.03\%$). The level of stiffness depression after shortening was similar ($12.3 \pm 2.70\%$) in both Ca^{2+} concentrations.

Experiments with MgADP. Figure 10A shows a typical experiment with three superimposed contractions produced in different SL by a fibre activated in $\text{pCa}^{2+}4.5$, in a solution containing 10 mM MgADP. As in the case of the experiments

using different pCa^{2+} , the forces produced after stretch and shortening were higher and lower, respectively, than the force produced during isometric contraction. MgADP did not affect the residual force enhancement or the force depression (Figure 10B). However stiffness after stretch did not increase in the presence of MgADP (Figure 11). When all experiments (Ca^{2+} and MgADP) are pooled, the relation between the history-dependence of force and stiffness is apparent (Figure 12), and shows that stiffness is affected by MgADP in the force enhanced state.

The stiffness measurements may be affected by compliance of the sarcomeres, and most specifically the compliance of the filaments. Although filament compliance may account for $\sim 50\%$ of the sarcomere compliance [37], its actual contribution to the strain-force relationship in a half-sarcomere is unknown. Isolated thick and thin filaments stretched from zero force to maximal physiological force develop strains of 0.3% and 1.5%, respectively [38,39], values that are too low for account for the changes in stiffness that we observed in this study. Most importantly, even if the compliance affects slightly the stiffness values that we obtained, there is no evidence that changes in Ca^{2+} concentration and MgADP affects the compliance of the filaments, and therefore the comparisons made throughout our study remain valid.

P_2 -to-peak/valley amplitude. In order to analyze the relationship between the force increase and decrease after stretch or shortening during phase 3 and the residual forces after length changes, we measured the relative distances between P_2 and the peak force during stretch, and between P_2 and the lowest force (valley) obtained during shortening. We noticed these distances were significantly greater in $\text{pCa}^{2+}6.0$ than in $\text{pCa}^{2+}4.5$, but they were not affected when MgADP was added to the solution (Figure 13).

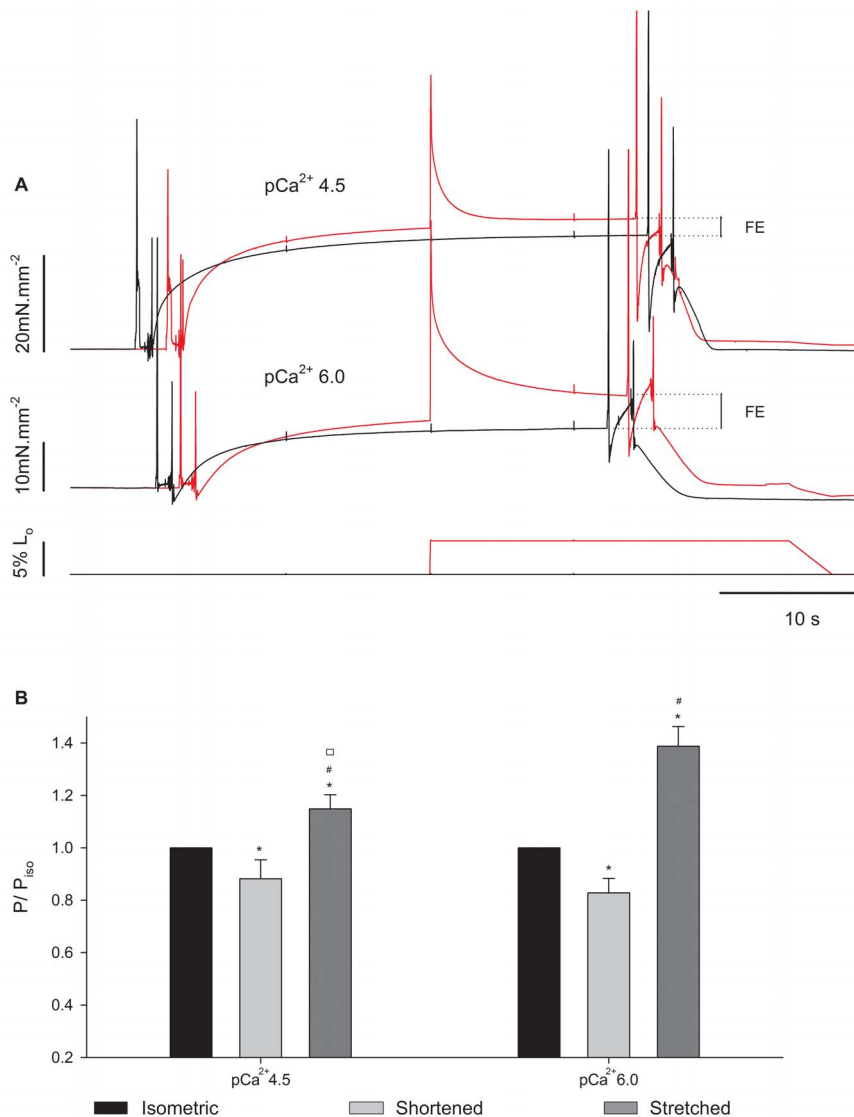


Figure 8. Residual force changes in different Ca²⁺ concentrations. (A) Sample records from a typical experiment showing superimposed contractions produced by a fibre activated in pCa²⁺4.5 and pCa²⁺6.0. Black: isometric contraction at SL of 2.8 μ m. Red: isometric contraction at SL of 2.65 μ m followed by a 5% stretch. The corresponding length changes are shown in the lower panels. (B) Mean (\pm S.E.M.) relative forces from fibres activated in pCa²⁺4.5 and pCa²⁺6.0 (n = 13) in three conditions: isometric (black bar), shortened (light grey bar) and stretched (dark grey bar). P = forces recorded 10 s after length changes; P_{iso} = force at the respective isometric condition. * significantly different from isometric, # significantly different from shortening, □ significantly different from the same condition (shortened) in pCa²⁺6.0. doi:10.1371/journal.pone.0068866.g008

Discussion

The main results of this study were that decreasing Ca²⁺ concentrations decreased the force produced during shortening and increased the force produced after stretch; these changes were accompanied by similar changes in stiffness. MgADP affected stiffness during shortening and after stretch, without concomitant changes in force. These results suggest that the mechanisms of force changes during stretch and shortening are different from those observed after the length changes, when forces have stabilized in a new steady-state.

Transient Forces during Length Changes

We detected differences in P₁ and L₁ resulting from changing Ca²⁺ concentrations during shortening, as previously shown (Minozzo et al, 2012). P₁ changes have been attributed mainly

to crossbridges engaging in specific states of the power-stroke during shortening [5,6,12]. In a previous study [5], we developed a model to better understand the effect of crossbridges biased into myosin.ADP.Pi (pre-power-stroke) complex on P₁. We observed that biasing crossbridges towards a pre-power-stroke state caused a decrease in isometric force and a decrease in P₁ during shortening. Although the experimental data in that study also showed a trend to decrease P₁ (figure 10 from Minozzo et al, 2012), the result was not statistically significant. In the current study, we observed that P₁ amplitude and L₁ were increased in pCa²⁺6.0. At lower Ca²⁺ concentrations, the absolute population of non-attached crossbridges is expected to be high; this population can affect the transition between non-force generating to force generating crossbridges via a cooperativity mechanism, which is more prominent in low than in saturating Ca²⁺ concentrations [40]. This interpretation is consistent with the experiments that showed

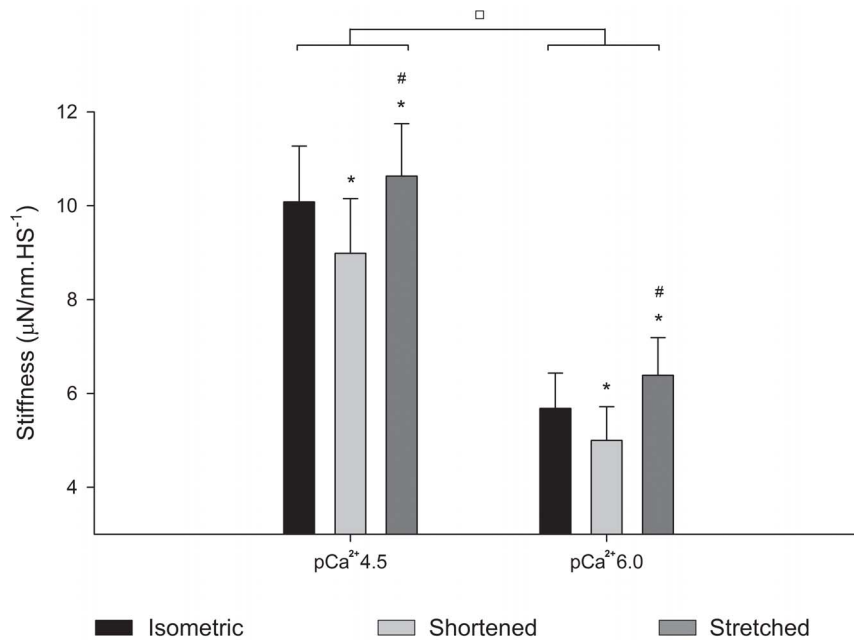


Figure 9. Mean stiffness after length changes. Mean stiffness values (\pm S.E.M) measured during isometric contractions (black bar), and when forces reach a new steady state after shortening (light grey bar) and stretch (dark grey bar) in experiments performed in pCa²⁺4.5 and pCa²⁺6.0. Decreasing Ca²⁺ concentration decreased the stiffness in all conditions. In both Ca²⁺ concentrations, the stiffness during stretch and shortening was higher and lower, respectively, than during isometric contractions. * Significantly different from isometric, # significantly different from shortening, □ significantly different from each other. doi:10.1371/journal.pone.0068866.g009

a direct relationship between stiffness and P₁ at different shortening velocities [6].

MgADP altered the relation between force development and stiffness during shortening by increasing only L₁, decreasing the stiffness/force ratio. MgADP not only induces myosin strong-binding to actin [41], which in turn would “turn-on” adjacent actin binding sites leading to myosin cooperativity [42], but also decreases the rigor stiffness without concomitant changes in force [43].

P₂ and L₂ during shortening were not affected by lowering the Ca²⁺ concentration. Assuming that P₂ and L₂ represent the critical force and length, respectively, at which crossbridges detach during shortening, our results are consistent with the rationale that the number of crossbridges formed before shortening does not change the relative strain necessary for their detachment [5].

The values of P₂ and L₂ were not affected by Ca²⁺ concentration during stretch. While one previous study showed an increase in P₂ when Ca²⁺ was elevated [4], and associated the increase to an enhanced stiffness/force ratio, another study [44] showed an increase in the stretch forces when Ca²⁺ was lowered from pCa²⁺4.5 to pCa²⁺6.3; these authors linked their result to a greater reliance on the rate of crossbridge detachment in low Ca²⁺ concentrations. Since the relative stiffness changes were not affected by Ca²⁺ concentrations, the stiffness increase during stretch did not follow the force increase, suggesting the later does not occur due to an increase in the number of crossbridges attached to actin. Instead, it suggests that the force increase during stretch can be caused either by an increase in force produced per crossbridge, or by pre-power-stroke crossbridges resisting to stretch [4,11]. Therefore our results are in line with our working hypothesis, which mainly attributes force changes during stretch to crossbridges in a pre-power-stroke state. These crossbridges would not contribute to isometric force generation, but would have the capacity to resist to stretch.

Residual Force Enhancement

Contrary to our hypothesis, the residual force enhancement was ~2.6-fold larger in pCa²⁺6.0 than in pCa²⁺4.5. The effect of activation on the residual force enhancement is unclear. Rassier et al. [16] did not observed changes in the force enhancement in intact fibres isolated from the frog and activated with different frequencies of stimulation. However, Campbell and Moss [45] observed a greater relative force increase in a second stretch when two consecutive stretches were applied in pCa²⁺6.2 compared to pCa²⁺4.5. The authors suggested that the rate at which cycling crossbridges reach a steady state is considerably longer at lower Ca²⁺ concentrations. Considering that the residual force enhancement could be caused partially by an increase in the number of attached crossbridges, fibres activated at lower Ca²⁺ concentration would have a greater population of crossbridges available to attach after stretch, which in turn could be responsible for a higher force enhancement in lower Ca²⁺ concentrations.

If it is assumed that an increase in stiffness may be caused by an increase in the number of crossbridges attached to actin, MgADP might have eliminated this effect. Thus, a complementary mechanism to explain the increased residual force enhancement in low Ca²⁺ concentration must exist, since the stiffness did not increase as much as the force after stretch. Force enhancement has been also associated with activation of passive structures during stretch [46–50]. Titin stiffness may increase with increasing Ca²⁺ concentrations [51], leading to an increased force produced during stretch. While some studies showed an increased force when fibres lacking myosin-actin interaction were activated with Ca²⁺ [47,51] other studies [52,53] showed that titin may decrease stiffness with increasing Ca²⁺ concentration. Nevertheless, it is still tempting to speculate that the increase in titin stiffness with Ca²⁺ contributed to force enhancement.

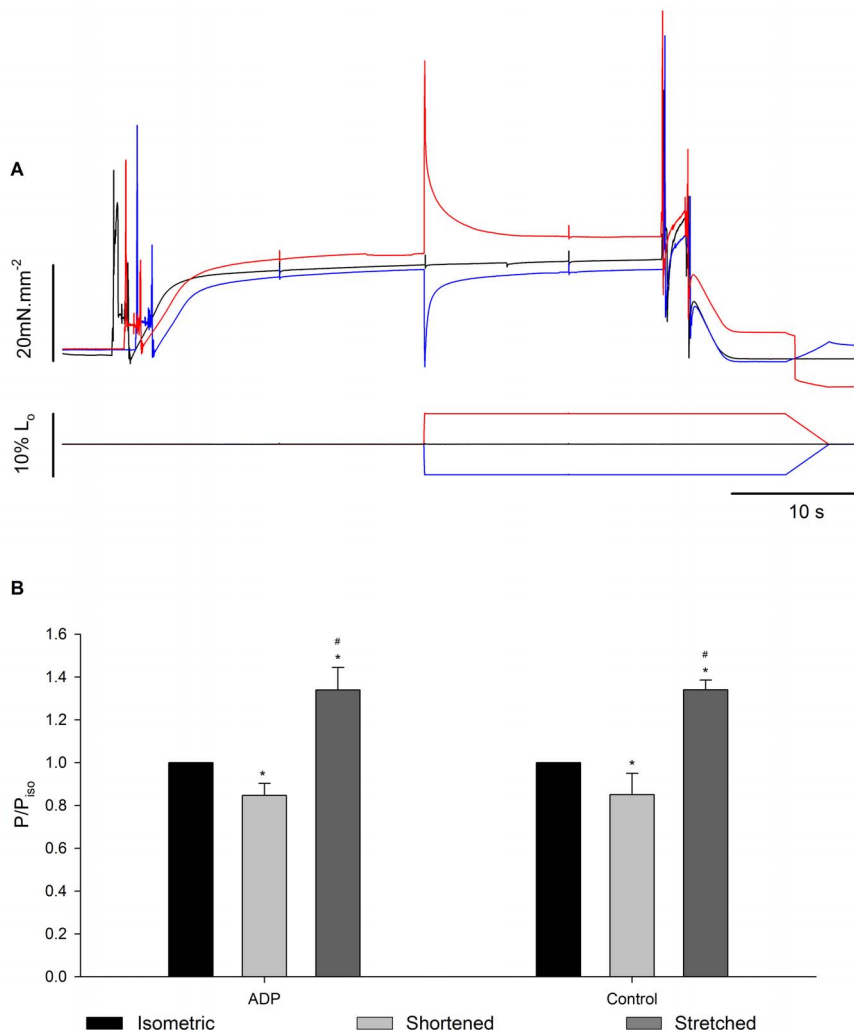


Figure 10. Residual force changes after MgADP treatment. (A) Sample records recorded during a typical experiment in a fibre activated in pCa²⁺4.5 with 10 mM MgADP. Black: isometric contraction at SL of 2.8 μ m. Red: isometric contraction at SL of 2.65 μ m followed by a 5% length stretch. Blue: isometric contraction at SL 2.95 μ m followed by a 5% length shortening. Lower panel: correspondent fibre length changes. (B) Mean (\pm S.E.M.) forces produced by fibres (n = 7) activated in pCa²⁺4.5 and pCa²⁺4.5+10 mM MgADP during isometric contractions (black bar), after shortening (light grey bar) and after stretch (dark grey bar). P = forces 10 s after length changes. P_{iso} = force produced during the respective isometric condition. * significantly different from isometric, # significantly different from shortening. doi:10.1371/journal.pone.0068866.g010

Finally, we cannot exclude that the residual forces after length changes may happen due to sarcomere/half-sarcomere length non-uniformity [50,54,55], a mechanism that would be also in line with the differences found when fibres were activated in different pCa²⁺. Accordingly, activation would lead to a population of sarcomeres that would elongate more, decreasing their amount of overlap until passive forces would emerge, while other sarcomeres would elongate less. The “weak” sarcomeres that would continuously elongate would reach a tension borne by passive elements that would equal the tension of the “strong”, shorter sarcomeres. It has been shown that myofibrils stretched at low Ca²⁺ concentrations presented more sarcomeres “yielding” (weakening) than at high Ca²⁺ concentration [56]. Assuming the same happened in our experiments, activation in pCa²⁺6.0 could have generated more sarcomere non-uniformity, causing a greater force enhancement than fibres activated in pCa²⁺4.5.

Residual Force Depression

The changes in stiffness accompanied the changes in force after shortening, suggesting a decrease in the number of attached crossbridges, as previously observed [18]. Force depression has been attributed to crossbridge inhibition caused by angular distortion of the actin binding sites induced by shortening after activation [15,17]. Changing Ca²⁺ concentrations did not change the residual force depression. This confirms our hypothesis that the number of crossbridges attached previously to shortening would not change the relative levels of force depression since the crossbridge inhibition mechanism is mainly dependent on the amount of new overlap zone formed between the two filaments after shortening.

The mechanisms proposing an inhibition of crossbridges attached in a newly overlap zone was strengthened in a previous study that we performed with isolated myofibrils (Pun et al. 2010). In that study the levels of force depression were decreased by MgADP activation, suggesting that activation via cooperativity counteracted part of the crossbridges inhibition caused by

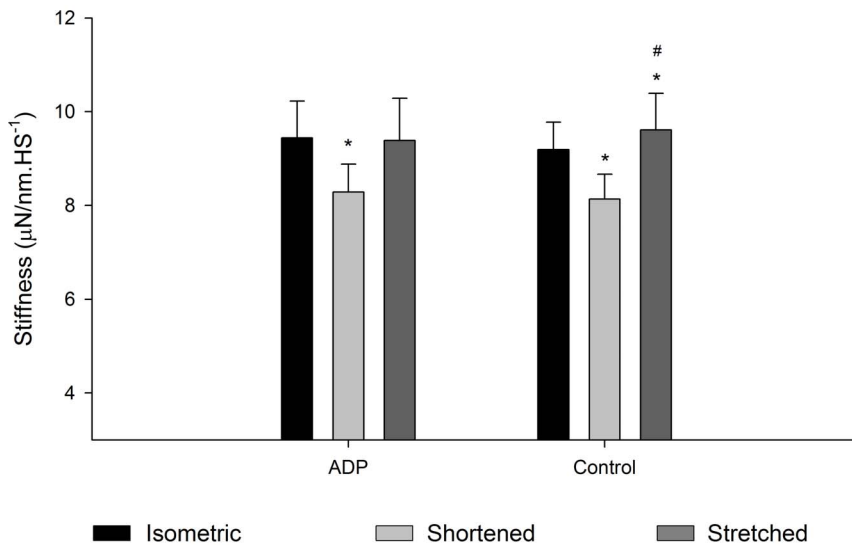


Figure 11. Mean stiffness after length changes. Mean stiffness values (\pm S.E.M) measured during isometric contractions (black bar), and when forces reach a new steady state after shortening (light grey bar) or stretch (dark grey bar) during experiments performed in pCa²⁺4.5 with and without MgADP (n = 7). * significantly different from isometric, # significantly different from shortening. doi:10.1371/journal.pone.0068866.g011

shortening. Differently, in the present study the residual force depression was not affected by MgADP activation. In the current study fibres were activated in saturating Ca²⁺ levels together with higher levels of MgADP (~4 times higher than in the previous study). In this situation, the role of myosin cooperativity in the force inhibition is likely decreased, as MgADP competes with MgATP for the myosin binding site; the more ATP the lesser the

influence of MgADP and cooperativity on fibre activation [41]. The reason MgADP was added to Ca²⁺ solution in the present study was that we did not want only to work with activation via cooperativity - in fact, we were interested in biasing a relatively large proportion of crossbridges into strong-bound states, expecting an opposite effect to what was previously observed with blebbistatin [4,5].

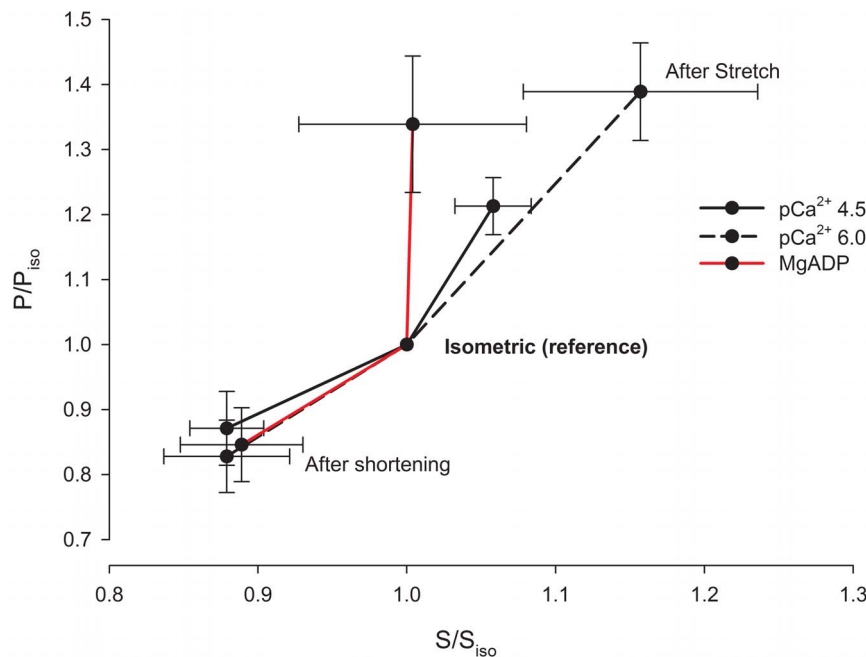


Figure 12. Relation between force and stiffness after length changes. Mean forces (P/P_{iso}±S.E.M.) plotted against the mean stiffness (S/S_{iso}±S.E.M.). Relative stiffness in MgADP after stretch does not follow the same trend as in Ca²⁺ solutions. P=force measured 10 s after length changes. P_{iso}=force at the respective isometric condition; S=stiffness measured 10 s after length changes in every condition, S_{iso}=stiffness at the respective isometric condition. doi:10.1371/journal.pone.0068866.g012

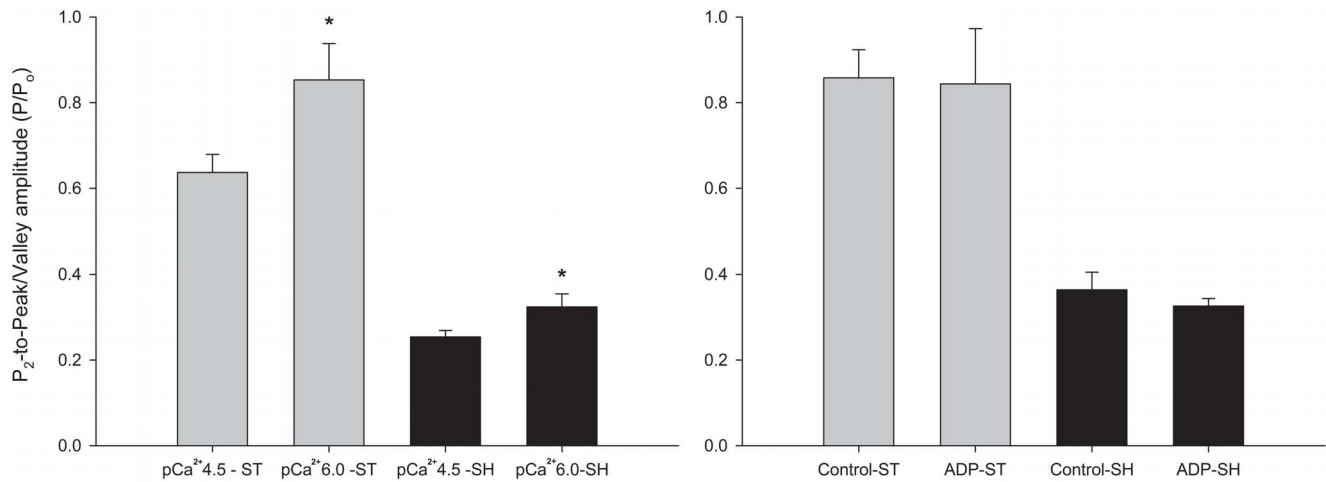


Figure 13. Difference between P₂ and forces at the end of length changes (peak for stretching and valley for shortening). Left panel: experiments performed in different pCa²⁺. Right panel: experiments performed with MgADP. ST = P/P_o during stretch (light gray bar), SH = P/P_o during shortening (black bar). * Significant difference between two groups. doi:10.1371/journal.pone.0068866.g013

Relation between the Transient Force and the Residual Forces

The relation between the force during and after length changes (phase 4) remains unclear. Edman and Tsuchiya [57] found a strong relationship between the level of force increase after P₂ and the level of residual force enhancement. They interpreted this first increase to a damping effect of “weak sarcomeres” working in parallel to elastic elements - this increase would be attenuated due to the release of elastic strain, but not cease after stretch. Assuming that fibres activated in low Ca²⁺ would allow more sarcomere “weakening” during and after stretch than at high Ca²⁺ concentration, one would expect that force increase after P₂ would also be increased when Ca²⁺ concentration is lowered. Conversely, assuming that MgADP did not affect SL non-uniformity, it would not alter the relation between these two

phases of force increase. We found that the levels of force enhancement after P₂ were accompanied by similar levels of force enhancement at different Ca²⁺ concentrations and when fibres were treated with MgADP. Nevertheless, the relative force decline during shortening was more pronounced at pCa²⁺6.0 than in pCa²⁺4.5. Considering thin filament deactivation the main mechanism for residual force depression [17], force decline after P₂ could only be partially attributed to this mechanism (see Roots et al. 2007). Apparently, distinct mechanisms are responsible also for force behavior after P₂ in stretch and shortening.

Author Contributions

Conceived and designed the experiments: FM DR. Performed the experiments: FM. Analyzed the data: FM DR. Contributed reagents/materials/analysis tools: DR. Wrote the paper: FM DR.

References

- Colombini B, Nocella M, Benelli G, Cecchi G, Griffiths PJ, et al. (2009) Reversal of the myosin power stroke induced by fast stretching of intact skeletal muscle fibers. *Biophys J* 97: 2922–2929.
- Ford LE, Huxley AF, Simmons RM (1977) Tension responses to sudden length change in stimulated frog muscle fibres near slack length. *J Physiol* 269: 441–515.
- Lombardi V, Piazzesi G (1990) The contractile response during steady lengthening of stimulated frog muscle fibres. *J Physiol* 431: 141–171.
- Minozzo FC, Rassier DE (2010) Effects of blebbistatin and Ca²⁺ concentration on force produced during stretch of skeletal muscle fibers. *Am J Physiol Cell Physiol* 299: C1127–1135.
- Minozzo FC, Hilbert L, Rassier DE (2012) Pre-Power-Stroke Cross-Bridges Contribute to Force Transients during Imposed Shortening in Isolated Muscle Fibers. *PLoS One* 7: e29356.
- Roots H, Offer GW, Ranatunga KW (2007) Comparison of the tension responses to ramp shortening and lengthening in intact mammalian muscle fibres: crossbridge and non-crossbridge contributions. *J Muscle Res Cell Motil* 28: 123–139.
- Bickham DC, West TG, Webb MR, Wolledge RC, Curtin NA, et al. (2011) Millisecond-scale biochemical response to change in strain. *Biophys J* 101: 2445–2454.
- Brunello E, Reconditi M, Elangovan R, Linari M, Sun YB, et al. (2007) Skeletal muscle resists stretch by rapid binding of the second motor domain of myosin to actin. *Proc Natl Acad Sci USA* 104: 20114–20119.
- Colomo F, Lombardi V, Piazzesi G (1986) A velocity-dependent shortening depression in the development of the force-velocity relation in frog muscle fibres. *J Physiol* 380: 227–238.
- Fusi L, Reconditi M, Linari M, Brunello E, Elangovan R, et al. (2010) The mechanism of the resistance to stretch of isometrically contracting single muscle fibres. *J Physiol* 588: 495–510.
- Getz EB, Cooke R, Lehman SL (1998) Phase transition in force during ramp stretches of skeletal muscle. *Biophys J* 75: 2971–2983.
- Ranatunga KW, Roots H, Pinniger GJ, Offer GW (2010) Crossbridge and non-crossbridge contributions to force in shortening and lengthening muscle. *Adv Exp Med Biol* 682: 207–221.
- Abbott BC, Aubert X (1952) The force exerted by active striated muscle during and after change of length. *J Physiol* 117: 77–86.
- Julian FJ, Morgan DL (1979) The effect on tension of non-uniform distribution of length changes applied to frog muscle fibres. *J Physiol* 293: 379–392.
- Pun C, Syed A, Rassier DE (2010) History-dependent properties of skeletal muscle myofibrils contracting along the ascending limb of the force-length relationship. *Proc Biol Sci* 277: 475–484.
- Rassier DE, Herzog W (2005) Relationship between force and stiffness in muscle fibres after stretch. *J Appl Physiol* 99: 1769–1775.
- Marechal G, Plaghki L (1979) The deficit of the isometric tetanic tension redeveloped after a release of frog muscle at a constant velocity. *J Gen Physiol* 73: 453–467.
- Sugi H, Tsuchiya T (1988) Stiffness changes during enhancement and deficit of isometric force by slow length changes in frog skeletal muscle fibres. *J Physiol* 407: 215–229.
- Herzog W, Leonard TR (2000) The history dependence of force production in mammalian skeletal muscle following stretch-shortening and shortening-stretch cycles. *J Biomech* 33: 531–542.
- Tsuchiya T, Sugi H (1988) Muscle stiffness changes during enhancement and deficit of isometric force in response to slow length changes. *Adv Exp Med Biol* 226: 503–511.
- Shimizu H, Fujita T, Ishiwata S (1992) Regulation of tension development by MgADP and Pi without Ca²⁺. Role in spontaneous tension oscillation of skeletal muscle. *Biophys J* 61: 1087–1098.

22. Edman KA (1996) Fatigue vs. shortening-induced deactivation in striated muscle. *Acta Physiol Scand* 156: 183–192.
23. Pinniger GJ, Ranatunga KW, Offer GW (2006) Crossbridge and non-crossbridge contributions to tension in lengthening rat muscle: force-induced reversal of the power stroke. *J Physiol* 573: 627–643.
24. Fabiato A (1988) Computer programs for calculating total from specified free or free from specified total ionic concentrations in aqueous solutions containing multiple metals and ligands. *Methods Enzymol* 157: 378–417.
25. Colombini B, Bagni MA, Palmiini RB, Cecchi G (2005) Crossbridge formation detected by stiffness measurements in single muscle fibres. *Adv Exp Med Biol* 565: 127–140.
26. Zhao Y, Kawai M (1994) Kinetic and thermodynamic studies of the cross-bridge cycle in rabbit psoas muscle fibers. *Biophys J* 67: 1655–1668.
27. Bershtitsky SY, Tsaturyan AK (2002) The elementary force generation process probed by temperature and length perturbations in muscle fibres from the rabbit. *J Physiol* 540: 971–988.
28. Radocaj A, Weiss T, Helsby WI, Brenner B, Kraft T (2009) Force-generating cross-bridges during ramp-shaped releases: evidence for a new structural state. *Biophys J* 96: 1430–1446.
29. Ranatunga KW (1996) Endothermic force generation in fast and slow mammalian (rabbit) muscle fibers. *Biophys J* 71: 1905–1913.
30. Bagni MA, Cecchi G, Colombini B (2005) Crossbridge properties investigated by fast ramp stretching of activated frog muscle fibres. *J Physiol* 565: 261–268.
31. Rack PM, Westbury DR (1974) The short range stiffness of active mammalian muscle and its effect on mechanical properties. *J Physiol* 240: 331–350.
32. Edman KA, Elzinga G, Noble MI (1978) Enhancement of mechanical performance by stretch during tetanic contractions of vertebrate skeletal muscle fibres. *J Physiol* 281: 139–155.
33. Rassier DE (2008) Pre-power stroke cross bridges contribute to force during stretch of skeletal muscle myofibrils. *Proc Biol Sci* 275: 2577–2586.
34. Edman KA (1975) Mechanical deactivation induced by active shortening in isolated muscle fibres of the frog. *J Physiol* 246: 255–275.
35. Rassier DE, Herzog W, Wakeling J, Syme DA (2003) Stretch-induced, steady-state force enhancement in single skeletal muscle fibers exceeds the isometric force at optimum fiber length. *J Biomech* 36: 1309–1316.
36. Edman KA, Caputo C, Lou F (1993) Depression of tetanic force induced by loaded shortening of frog muscle fibres. *J Physiol* 466: 535–552.
37. Huxley HE, Stewart A, Sosa H, Irving T (1994) X-ray diffraction measurements of the extensibility of actin and myosin filaments in contracting muscle. *Biophys J* 67: 2411–2421.
38. Liu X, Pollack GH (2002) Mechanics of F-actin characterized with micro-fabricated cantilevers. *Biophys J* 83: 2705–2715.
39. Neumann T, Fauver M, Pollack GH (1998) Elastic properties of isolated thick filaments measured by nanofabricated cantilevers. *Biophys J* 75: 938–947.
40. Fitzsimons DP, Patel JR, Campbell KS, Moss RL (2001) Cooperative mechanisms in the activation dependence of the rate of force development in rabbit skinned skeletal muscle fibers. *J Gen Physiol* 117: 133–148.
41. Fukuda N, Fujita H, Fujita T, Ishiwata S (1998) Regulatory roles of MgADP and calcium in tension development of skinned cardiac muscle. *J Muscle Res Cell Motil* 19: 909–921.
42. Bremel RD, Weber A (1972) Cooperation within actin filament in vertebrate skeletal muscle. *Nat New Biol* 238: 97–101.
43. Dantzig JA, Barsotti RJ, Manz S, Sweeney HL, Goldman YE (1999) The ADP release step of the smooth muscle cross-bridge cycle is not directly associated with force generation. *Biophys J* 77: 386–397.
44. Stienen GJ, Versteeg PG, Papp Z, Elzinga G (1992) Mechanical properties of skinned rabbit psoas and soleus muscle fibres during lengthening: effects of phosphate and Ca²⁺. *J Physiol* 451: 503–523.
45. Campbell KS, Moss RL (2002) History-dependent mechanical properties of permeabilized rat soleus muscle fibers. *Biophys J* 82: 929–943.
46. Bagni MA, Colombini B, Geiger P, Berlinguer PR, Cecchi G (2004) Non-cross-bridge calcium-dependent stiffness in frog muscle fibers. *Am J Physiol Cell Physiol* 286: C1353–1357.
47. Cornachione AS, Rassier DE (2012) A non-cross-bridge, static tension is present in permeabilized skeletal muscle fibers after active force inhibition or actin extraction. *Am J Physiol Cell Physiol* 302: C566–574.
48. Leonard TR, Herzog W (2010) Regulation of muscle force in the absence of actin-myosin-based cross-bridge interaction. *Am J Physiol Cell Physiol* 299: C14–20.
49. Herzog W, Leonard TR (2002) Force enhancement following stretching of skeletal muscle: a new mechanism. *J Exp Biol* 205: 1275–1283.
50. Rassier DE (2012) The mechanisms of the residual force enhancement after stretch of skeletal muscle: non-uniformity in half-sarcomeres and stiffness of titin. *Proc Biol Sci* 279: 2705–2713.
51. Labeit D, Watanabe K, Witt C, Fujita H, Wu Y, et al. (2003) Calcium-dependent molecular spring elements in the giant protein titin. *Proc Natl Acad Sci USA* 100: 13716–13721.
52. Stuyvers BD, Miura M, Jin JP, ter Keurs HE (1998) Ca²⁺-dependence of diastolic properties of cardiac sarcomeres: involvement of titin. *Prog Biophys Mol Biol* 69: 425–443.
53. Yamasaki R, Berri M, Wu Y, Trombitas K, McNabb M, et al. (2001) Titin-actin interaction in mouse myocardium: passive tension modulation and its regulation by calcium/S100A1. *Biophys J* 81: 2297–2313.
54. Edman KA (2012) Residual force enhancement after stretch in striated muscle. A consequence of increased myofilament overlap? *J Physiol* 590: 1339–1345.
55. Morgan DL (1994) An explanation for residual increased tension in striated muscle after stretch during contraction. *Exp Physiol* 79: 831–838.
56. Shimamoto Y, Suzuki M, Mikhailenko SV, Yasuda K, Ishiwata S (2009) Intersarcomere coordination in muscle revealed through individual sarcomere response to quick stretch. *Proc Natl Acad Sci USA* 106: 11954–11959.
57. Edman KA, Tsuchiya T (1996) Strain of passive elements during force enhancement by stretch in frog muscle fibres. *J Physiol* 490 (Pt 1): 191–205.